Electrical conduction mechanism in a-$Se_{80-x}Te_xGa_{20}$ films (0<or=x<or=20)

1995 J. Phys.: Condens. Matter 7 8979

(http://iopscience.iop.org/0953-8984/7/47/017)

J. Phys.: Condens. Matter 7 (1995) 8979–8991. Printed in the UK

Electrical conduction mechanism in a-$Se_{80-x}Te_xGa_{20}$ films ($0 \leqslant x \leqslant 20$)

Zishan H Khan†, M Manzar Malik‡, M Zulfequar† and M Husain†

† Department of Physics, Jamia Millia Islamia, New Delhi-110 025, India

‡ Department of Physics, Maulana Azad College of Technology, Bhopal, India

Received 20 February 1995, in final form 16 August 1995

Abstract. The dark conductivity and transient photoconductivity measurements on thin films of a-$Se_{80-x}Te_xGa_{20}$ ($0 \leqslant x \leqslant 20$) have been reported in the temperature range from 148 to 318 K. The results indicate that, at higher temperatures, hopping conduction takes place in the tail states. At lower temperatures the conduction is due to variable-range hopping, which is in fair agreement with the Mott condition of variable-range hopping. The transient photoconductivity measurements show non-exponential decay, and recombination in these glasses may be considered to take place through the valence and conduction bands.

1. Introduction

Chalcogenide glasses have attracted great attention because of their use in various solid state devices, such as switching and memory, image converters and optical mass memories. The effect of impurities on the electrical properties has been a controversial issue since the discovery of these glasses.

In the present work, we report studies on the electrical transport properties of Se–Te alloys. Se is an important material and widely used to photographic drums, but in a pure state it does have disadvantages because of its short lifetime and low sensitivity. Se–Te alloys are useful due to their greater hardness, higher photosensitivity, higher crystallization temperature and small aging effects compared to the pure amorphous selenium. It has also been pointed out [1] that Se–Te alloys have extra advantages over amorphous Se as far as their use in xerography is concerned. Various workers [2, 3] have studied the effect of incorporation of various elements (S, Te, Bi, As and Ge) on the structure of glassy Se by infrared, Raman spectroscopy and thermal studies. The early studies [4, 5] show that these glasses are insensitive to impurities. However, later experiments show that the impurity effect does exist in chalcogenide glasses [6–9]. This shows that some impurity atoms may be situated in sites with an unusual configuration which do not allow their valencies to be satisfied and they therefore behave in an electrically active manner and can be donors or acceptors. Therefore, the effect of an impurity in chalcogenide glasses depends upon the composition of the glasses, the chemical nature of the impurity, the method of doping and the impurity concentration. We have chosen gallium as an additive material because it appears to be a quick hardener when added to pure selenium. It is also a typical metal having a low melting point (28 °C) and a very high boiling point (2403 °C). Recently, gallium was used in doping semiconductors and producing solid state devices. Moreover, gallium readily alloys with most metals and has been used as a component of low-melting alloys. It has

0953-8984/95/478979+13$19.50

also become an attractive material as a substrate because of its good lattice matching with solid solutions of III–VI compound semiconductors, which are useful for the fabrication of solid state devices. Several workers [10, 11] have conducted electrical as well as structural studies of Ga–Se binary alloys in the amorphous state.

The present communication reports the effect of the incorporation of Te on the dark conductivity and transient photoconductivity in vacuum-evaporated thin films of $Se_{80-x}Te_xGa_{20}$ ($0 \leqslant x \leqslant 20$).

2. Experimental details

Glassy alloys of $Se_{80-x}Te_xGa_{20}$ ($x = 0, 5, 10, 15$ and 20) were prepared by the quenching technique. Pure materials (99.999%) were sealed in quartz ampoules (length, about 5 cm; internal diameter, about 8 mm) in a vacuum of about 10^{-5} Torr. The sealed ampoules were kept inside a furnace where the temperature was raised to 700 °C at a rate of 3–4 °C min^{-1}. The ampoules were frequently rocked for 10 h at a temperature of 700 °C to make the melt homogeneous. The quenching was done in ice–water. The glassy nature of these alloys was verified by x-ray diffraction. Thin films of the glassy alloys of $Se_{80-x}Ga_{20}Te_x$ ($0 \leqslant x \leqslant 20$) were prepared by vacuum evaporation, keeping the substrates at room temperature and at a base pressure of about 10^{-5} Torr. The films were kept inside the vacuum chamber for 24 h to attain metastable equilibrium as suggested by Abkowitz [12]. Pre-deposited thick indium electrodes on a well degassed glass substrate were used for electrical contact. Planar geometry (length, about 1.5 cm; electrode gap, about 0.06 cm; thickness, about 5000 Å) of the films was used for conductivity measurements. The measurements were made in the vacuum of about 10^{-3} Torr. The temperature was measured with calibrated copper–constantan thermocouples mounted near the electrodes. For the electrical conductivity measurements, a voltage of 1.5 V (from a dry cell) was applied across the planar films and the resulting current was measured with a Keithley electrometer (model 617). A specially designed metallic cryostat was used to measure the dark conductivity and the transient photoconductivity of the thin films. A tungsten lamp (100 W) was used to irradiate the samples. The desired temperature in the cryostat was maintained using liquid nitrogen for low-temperature measurements. The error during the measurements was about ±1%.

Table 1. Electrical parameters in a-$Se_{80-x}Te_xGa_{20}$ for the temperature range 287–318 K.

Sample	σ_{DC} (at 310 K) (Ω^{-1} cm^{-1})	ΔE (eV)	σ_0 (Ω^{-1} cm^{-1})	σ_{ph}/σ_d (at 287 K) (10^8 lux)
$Se_{80}Ga_{20}$	8.19×10^{-6}	0.31	0.890	0.84
$Se_{75}Ga_{20}Te_5$	3.39×10^{-5}	0.22	0.130	0.23
$Se_{70}Ga_{20}Te_{10}$	1.79×10^{-6}	0.15	4.88×10^{-4}	0.33
$Se_{65}Ga_{20}Te_{15}$	6.68×10^{-5}	0.07	9.16×10^{-4}	0.49
$Se_{60}Ga_{20}Te_{20}$	8.04×10^{-3}	0.04	3.59×10^{-2}	0.03

3. Results and discussion

3.1. Dark conductivity

Figure 1 shows the temperature dependence of the dark conductivity of a-$Se_{80-x}Te_xGa_{20}$ films. In all the samples, the plots of ln σ_{DC} versus 1000/T are straight lines, indicating

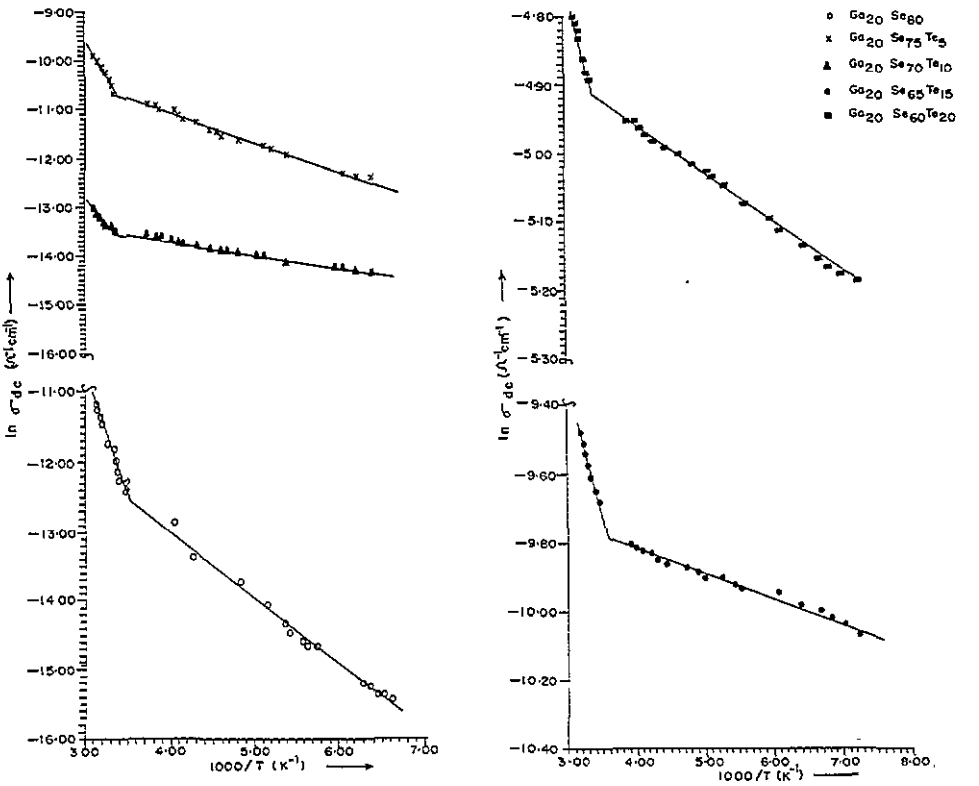

Figure 1. Temperature dependence of the DC conductivity in the temperature range 148–318 K at various concentrations of Te in the $Se_{80-x}Te_xGa_{20}$ system.

that the conduction in these glasses is through an activated process in the temperature range 287–318 K. The DC conductivity σ_{DC} can, therefore, be expressed by the usual relation

$$\sigma_{DC} = \sigma_0 \exp(-\Delta E/kT) \tag{1}$$

where ΔE is the activation energy for DC conduction, k is the Boltzmann constant and σ_0 is the pre-exponential factor. Table 1 shows the calculated values of activation energy ΔE and pre-exponential factors σ_0. From the calculated values of activation energy ΔE and pre-exponential factor σ_0, one can suggest that the conduction is due to the hopping of charge carriers in the tail states. Figure 2 shows the variation in dark conductivity and activation energy with Te concentration for the temperature region 287–318 K. The DC conductivity increases from 8.19×10^{-6} to 8.04×10^{-3} Ω^{-1} cm^{-1} as the concentration of Te increases. An increase in dark conductivity with a corresponding decrease in the activation energy is found to be associated with the shift of the Fermi level for the impurity-doped chalcogenide glasses [1, 9]. However, it has also been pointed out that the increase in conductivity could be caused by the increase in the portion of hopping conduction through defect states associated with the impurity atom [9]. The activation energy ΔE alone does not provide any information as to whether the conduction takes place in the extended states above the mobility edge or by hopping in the localized states. Both these conduction mechanisms occur simultaneously, with conduction via localized states dominating at low temperatures. The activation energy in the former case represents the energy difference between the mobility edge and the Fermi level. In the latter case, it represents the sum of

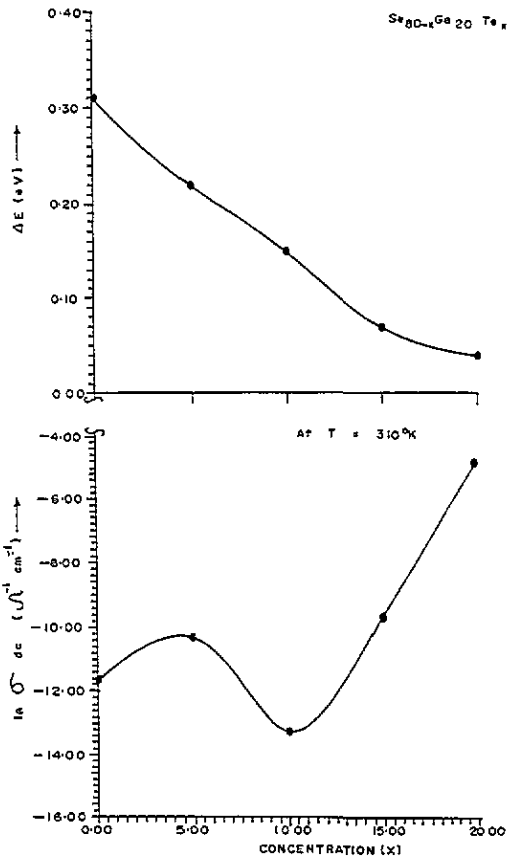

Figure 2. Concentration x versus ln σ_{DC} in a-$Se_{80-x}Te_xGa_{20}$ at a temperature of 310 K, and concentration x versus ΔE in a-$Se_{80-x}Te_xGa_{20}$ (287–318 K).

the energy separation between the occupied localized states and Fermi level and the mobility activation energy between the localized states for the hopping process.

These two conduction mechanisms can be distinguished on the basis of the pre-exponential factor σ_0. It was suggested by Mott [13] that the pre-exponential factor σ_0 (of equation (1)) for conduction in the localized states should be two or three orders smaller in magnitude than for conduction in the extended states and should become still smaller for conduction in the localized states near the Fermi level. The values of σ_0 reported for a-Se and other Se alloyed films are of the order of $10^4\ \Omega^{-1}\ cm^{-1}$ [14] for conduction in the extended states, while in the present system the values of σ_0 decrease to $10^{-4}\ \Omega^{-1}\ cm^{-1}$. Therefore, the possibility of extended-state conduction is completely ruled out and hopping conduction in the tail states [15] is likely to take place. The low value of the pre-exponential factor σ_0 (about 10^{-3}) for the a-Se–Te system has already been reported by Mishra *et al* [20]. The value of ΔE decreases, which implies that either there is a large decrease in the band gap of the a-$Se_{80-x}Te_xGa_{20}$ system ($0 \leqslant x \leqslant 20$) or the width of the localized states increases.

The plot of ln σ_{DC} versus 1000/T in the high-temperature region (287–318 K) is linear, while a kink is observed at a temperature of about 278 K, below which the plot deviates from linearity. Therefore, the low-temperature data for these films have been replotted as

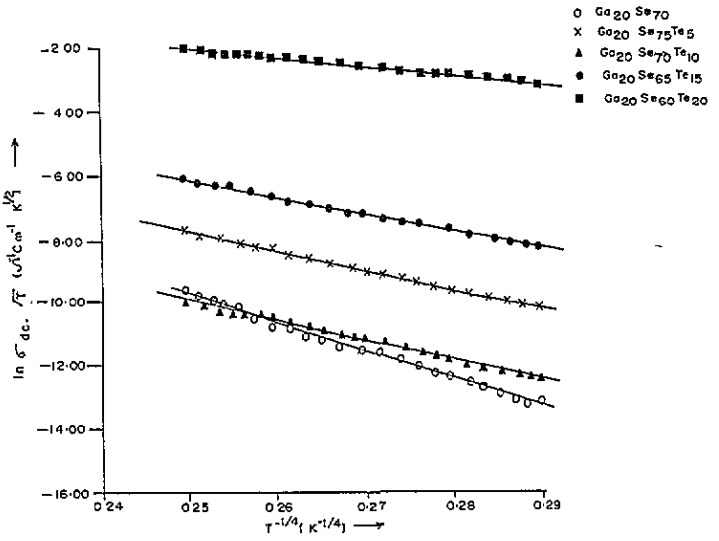

Figure 3. ln $\sigma_{DC}\sqrt{T}$ versus $T^{-1/4}$ at various concentrations of Te in the a-$Se_{80-x}Te_xGa_{20}$ system.

Table 2. The Mott parameters for a-$Se_{80-x}Te_xGa_{20}$.

x (% Te)	A ($K^{1/4}$)	T_0 (K)	σ_0' (Ω^{-1} cm^{-1})	α (cm^{-1})	R (cm) (at 260 K)	$N(E_F)$ (eV^{-1} cm^{-3})	W (meV) (at 260 K)	αR
0	82.50	4.65×10^7	46.65×10^3	7.15×10^9	1.11×10^{-9}	1.47×10^{27}	118.81	7.94
5	64.25	1.53×10^7	3.12×10^3	2.90×10^8	2.13×10^{-8}	2.66×10^{23}	92.92	6.18
10	62.52	1.73×10^7	1.31×10^2	1.15×10^7	5.23×10^{-7}	1.86×10^{19}	89.77	6.02
15	50.15	6.33×10^6	2.91×10^2	1.65×10^7	2.93×10^{-7}	1.31×10^{20}	72.49	4.84
20	29.15	7.22×10^5	1.77×10^2	3.39×10^6	8.29×10^{-7}	9.99×10^{18}	41.97	2.81

Table 3. The Mott parameters for a-$Se_{80-x}Te_xGa_{20}$, taking $\alpha = 10^7$ cm^{-1}.

x (% Te)	A ($K^{1/4}$)	T_0 (K)	σ_0' (Ω^{-1} cm^{-1})	R (cm)	$N(E_F)$ (eV^{-1} cm^{-3})	W (meV)	αR
0	82.5	4.65×10^7	46.65×10^3	7.95×10^{-7}	4.01×10^{18}	118.55	7.95
5	64.25	1.73×10^7	3.12×10^3	6.19×10^{-7}	1.09×10^{19}	92.39	6.19
10	62.52	1.53×10^7	1.31×10^2	6.02×10^{-7}	1.22×10^{19}	89.74	6.02
15	50.15	6.33×10^6	2.91×10^2	4.83×10^{-7}	2.92×10^{19}	72.35	4.83
20	29.15	7.22×10^5	1.77×10^2	2.81×10^{-7}	2.57×10^{20}	41.89	2.81

ln $\sigma_{DC}\sqrt{T}$ versus $T^{-1/4}$ (figure 3).

Table 1 shows the high-temperature conductivity data for a-$Se_{80-x}Te_xGa_{20}$ (where $0 \leqslant x \leqslant 20$), which confirms the thermally assisted tunnelling of charge carriers due to hopping in the tail states. The conductivity in low-temperature region (148–287 K) increases very slowly with increasing temperature, which suggests that conduction is due to variable-range hopping in localized states near the Fermi level. It may be mentioned here that, when sufficient phonon energy is available, the hopping is thermally assisted and is between the nearest neighbours in accordance with equation (1). On the other hand,

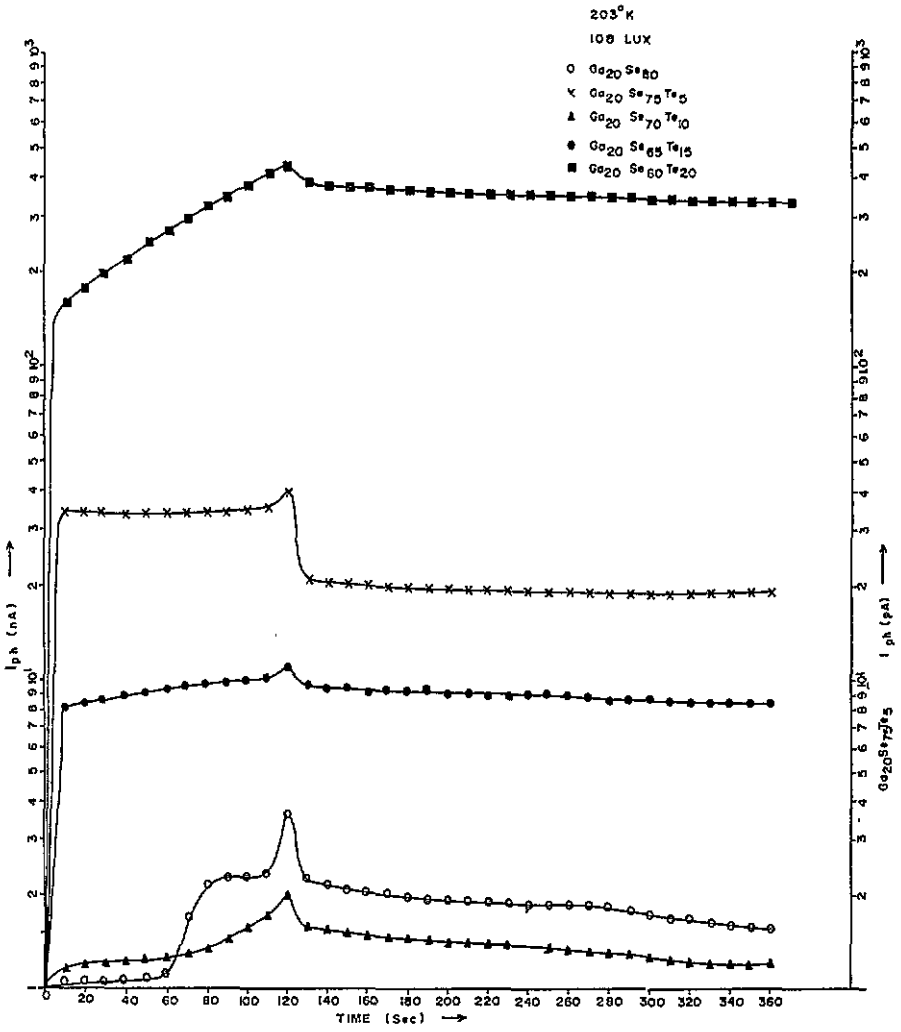

Figure 4. Rise and decay of photocurrent at 203 K in a-$Se_{80-x}Te_xGa_{20}$.

when the phonon energy is insufficient, the more energetic phonon-assisted hops become favourable, as a result of which the carriers will tend to hop a larger distance in order to locate sites which are energetically closer than the nearest neighbours. This variable-range hopping mechanism is characterized by the Mott [15] expression of the form

$$\sigma(T) = \frac{\sigma_0'}{\sqrt{T}} \exp(-AT^{-1/4}) \tag{2}$$

where

$$A^4 = T_0 = \frac{\lambda\alpha^3}{kN(E_F)} \tag{3}$$

$N(E_F)$ is the density of localized states at E_F, λ is a dimensionless constant (about 18), α^{-1} represents the spatial extension of the wavefunction $\exp(-\alpha R)$ associated with the localized states and k is the Boltzmann constant. The value of σ_0' as obtained by various

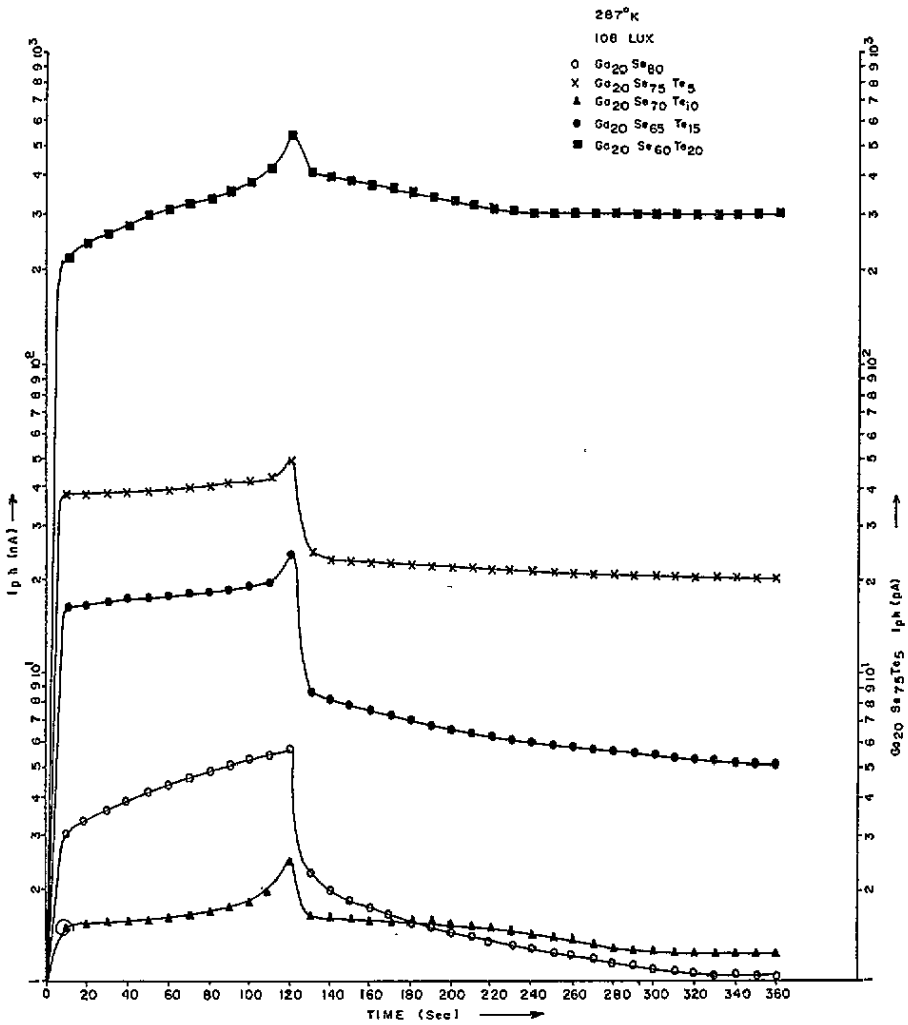

Figure 5. Rise and decay of photocurrent at 287 K in a-$Se_{80-x}Te_xGa_{20}$.

workers [14–19] is given by

$$\sigma_0' = 3e^2\gamma\left(\frac{N(E_F)}{8\pi\alpha kT}\right)^{1/2} \tag{4}$$

where e is the electron charge and γ is the Debye frequency (about 10^{13} Hz) [14]. Simultaneous solution of (3) and (4) yields

$$\alpha = 22.52\sigma_0'A^2 \text{ cm}^{-1} \tag{5}$$

and

$$N(E_F) = 2.12 \times 10^9\sigma_0'^3A^2 \text{ cm}^{-3} \text{ eV}^{-1}. \tag{6}$$

The hopping distance is given by [15]

$$R = \left(\frac{9}{8\pi\alpha kTN(E_F)}\right)^{1/4} \tag{7}$$

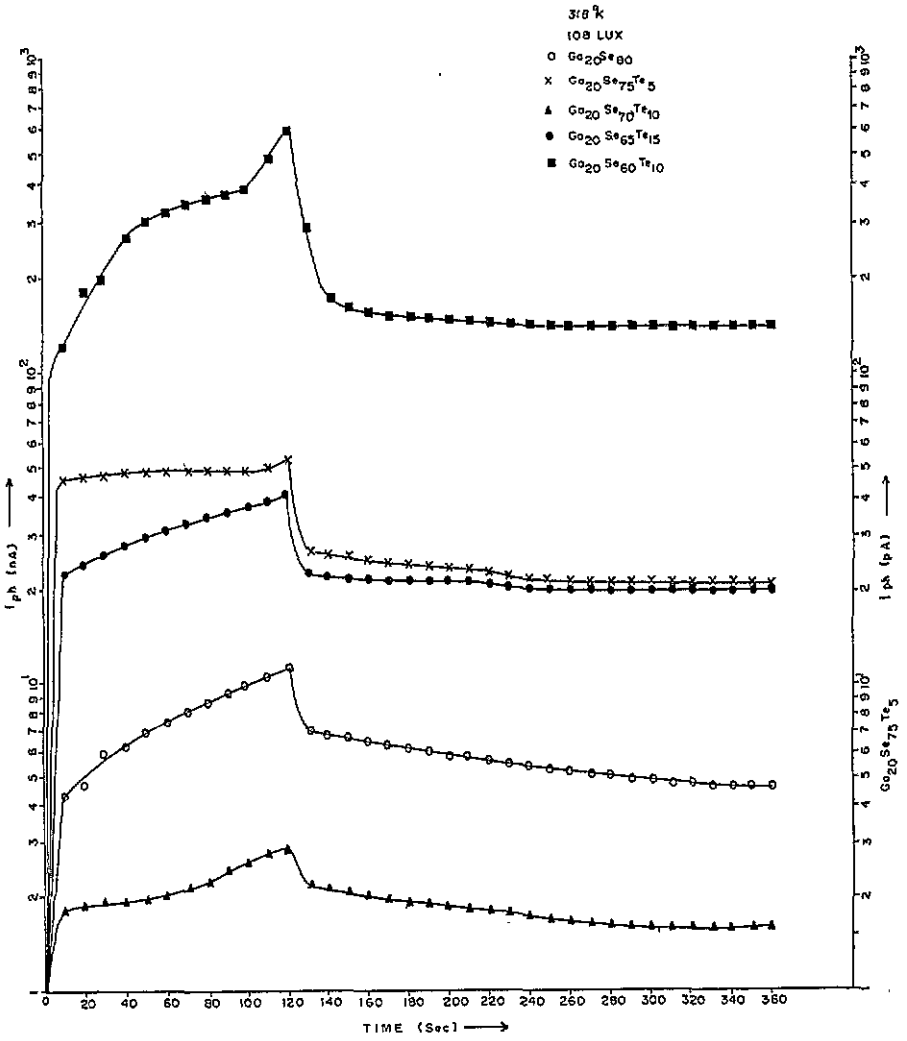

Figure 6. Rise and decay of photocurrent at 318 K in a-$Se_{80-x}Te_xGa_{20}$.

and hopping energy is also given by [15]

$$W = \frac{3}{4\pi R^3 N(E_F)}. \tag{8}$$

It may be mentioned that it is difficult to distinguish between equations (1) and (2) on the basis of the observed conductivity–temperature variation. The only possible distinction that can be made is on the basis of the value of W and αR, which according to Mott [15] should have values greater than kT and unity, respectively, for variable-range hopping conduction. Various Mott parameters A, σ_0', $N(E_F)$, T_0, α, W and αR are calculated using equations (2)–(8) and are given in table 2. It is found that the values of T_0, W and α decrease with increasing Te concentration. Since T_0 represents the degree of disorder and α^{-1} the degree of localization, it follows that the amorphicity of the samples decreases with increasing Te concentration. The Mott formula, however, yields unreasonable results (table 2) such as $N(E_F) = 10^{27}$ and 10^{23} eV^{-1} cm^{-3}, respectively, for $Se_{80}Ga_{20}$ and

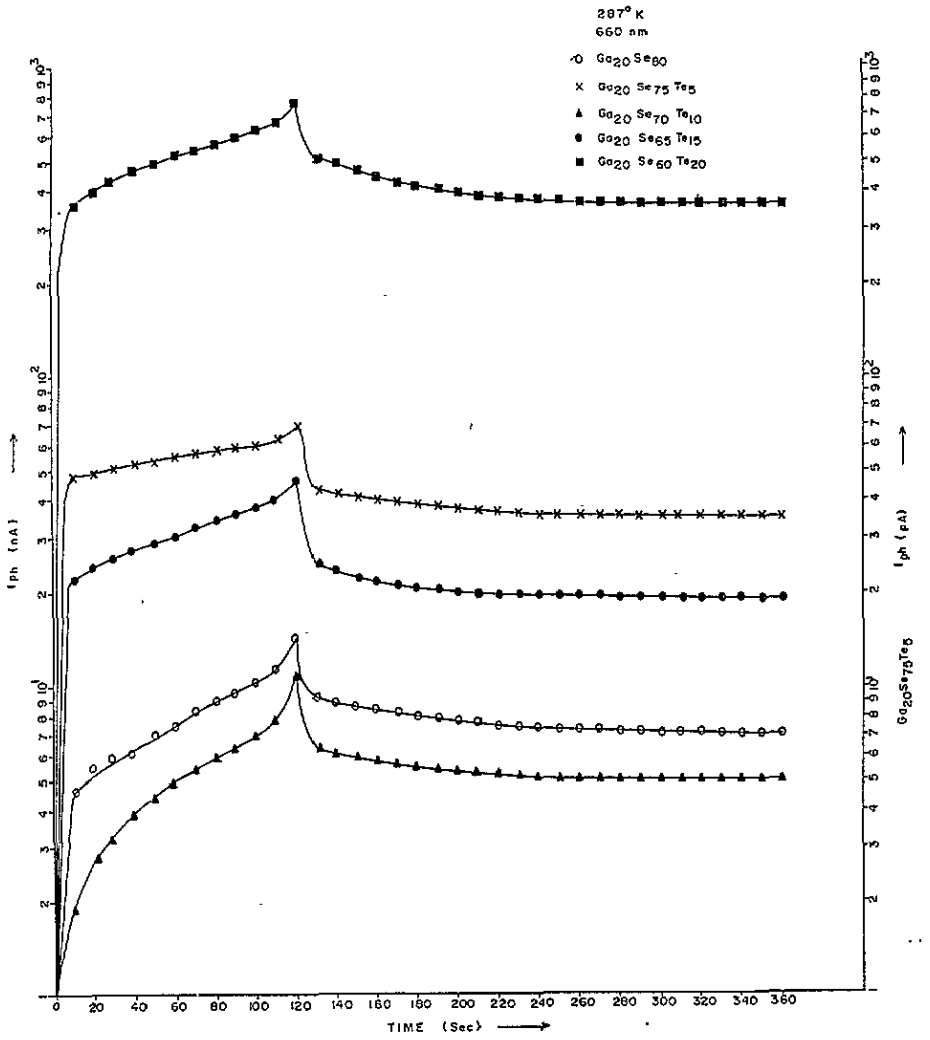

Figure 7. Rise and decay of photocurrent at a wavelength of 660 nm and at 287 K in a-$Se_{80-x}Te_xGa_{20}$.

$Se_{70}Te_{10}Ga_{20}$. Such discrepancies in the Mott formulation have also been reported by other workers [19, 21]. Brodsky and Gambino [22], however, removed this discrepancy to some extent by assuming the constant value of α^{-1} to be 5 Å. They reported a localized-state density of 2×10^{19} eV^{-1} cm^{-3} for a-Ge films. Therefore in the present case the Mott parameters [23] have been recalculated by taking a constant value of α equal to 10^7 cm^{-1} (table 3) and these results are similar to those obtained by other workers on chalcogenide glasses. It is evident from table 3 that the localized-state density $N(E_F)$ increases from 10^{18} to 10^{20} with increasing Te concentration. Tellurium glass contains short chains, while Se glass contains a mixture of long chains and Se rings. As the Te concentration increases, the number of Se rings decreases and the number of long Se–Te polymeric chains and Se–Te mixed rings increases [3]. It has also been pointed out [24] that the density of localized states increases as the Te concentration increases in the a-Se–Te system. The electron affinity

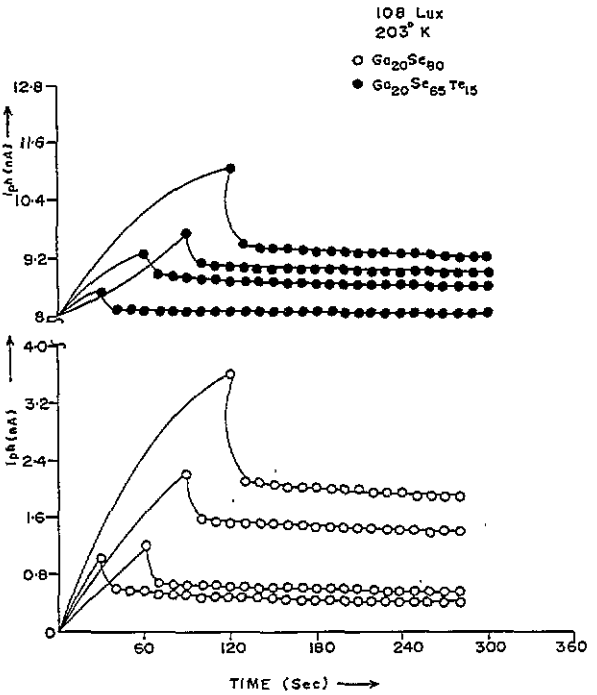

Figure 8. I_{ph} versus time t at various illumination time (t = 30, 60, 90 and 120 s).

of the Te atom is lower than that of Se, and no Te atom is mixed in Se atom chains and therefore could not act as an ionized impurity [25]. For this reason, the degree of disorder decreases and the density of defect states increases on incorporating Te in the a-Se–Te–Ga system. These results are in good agreement with the results obtained by other workers for amorphous films [26–28]. It may also be mentioned here that the magnitude of T_0/T [29] should be higher by two or three orders for amorphous films than for polycrystalline films [30], and this has been observed in the present system of a-$Se_{80-x}Te_xGa_{20}$ (where $0 \leqslant x \leqslant 20$). Therefore, it can be concluded that the Ga content present in the a-$Se_{80-x}Te_xGa_{20}$ ($x = 20$) crystallizes, thereby making the film less amorphous. Gallium has a more pronounced effect on conductivity as the number of long Se–Te polymeric chains and Se–Te mixed rings increases [3]. It is also evident from tables 2 and 3 that the values of W and αR are almost equal irrespective of the value of α, which may be evaluated with the help of the Mott pre-exponential factor σ_0' or can be assumed constant [15]. At low temperatures, we have calculated the hopping energy W. The order of W is inconsistent with the results of the other workers [31]. Thus, the present observations are in fair agreement with the Mott condition of variable-range hopping conduction, because $W \approx 4kT$ and $\alpha R \approx 6.0$. From the above discussion, one is led to the conclusion that, at higher temperatures, hopping conduction is taking place in the band tails of localized states and at lower temperatures the conduction is due to variable-range hopping with a kink at a temperature of about 278 K.

3.2. Photoconductivity

Figures 4–7 show the rise and decay of the photocurrent in a-$Se_{80-x}Te_xGa_{20}$. Transient photoconductivity measurements have been made at different temperatures (203, 287 and

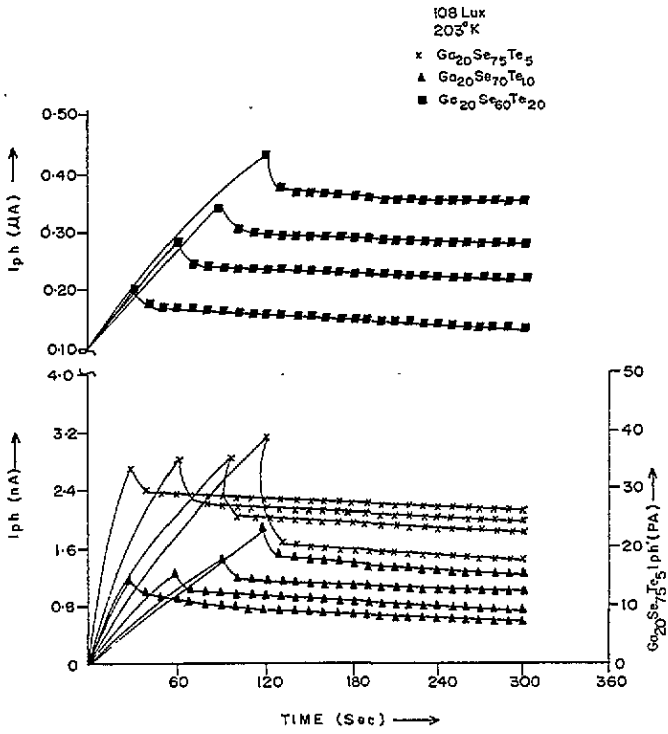

Figure 9. I_{ph} versus time t at various illumination time ($t = 30$, 60, 90 and 120 s).

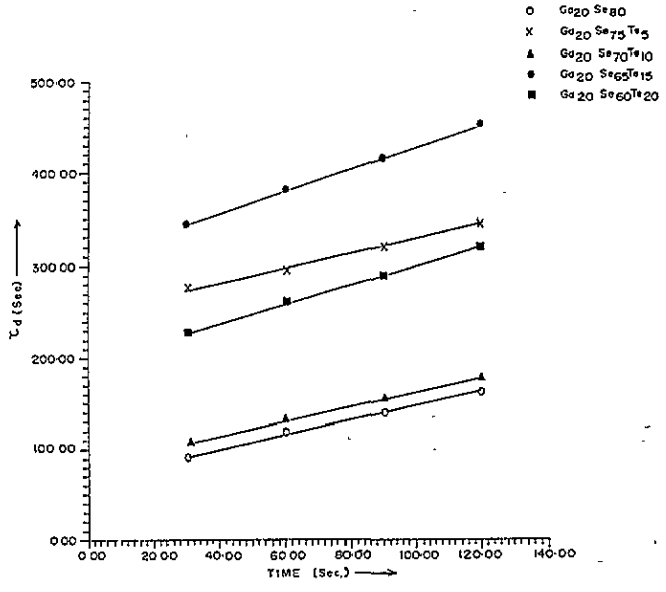

Figure 10. Differential lifetime τ_d versus time t at 203 K in a-$Se_{80-x}Te_xGa_{20}$.

318 K) using white light. The plots of I_{ph} versus time at temperatures (203, 287 and 318 K) show that the photocurrent at all temperatures and at a particular intensity (108 lux) increases

with time. These specimens at all temperatures show non-exponential decay [32]. The persistent photocurrent and slow decay are observed for all specimens at all temperatures; this may be due to carriers trapped in localized states. The photocurrent does not reach zero after decaying for a very long time (4 min) after the incident radiation is switched off. The light exposure of all the samples remained for 2 min. Several workers [33, 34] have reported the persistent photocurrent and slow decay in various other amorphous semiconductors. Transient photoconductivity measurements have also been made at a wavelength of 660 nm and at a temperature of 287 K (figure 7). The rise and decay of photocurrent at this particular wavelength are of the same nature as observed in white light, but only the magnitude of the photocurrent becomes large.

To study the decay rate at various temperatures and illumination times, we have used the differential lifetime concept as suggested by Fuch and Mayer [33] which is given by

$$\tau_d = -[(1/I_{ph})(\mathrm{d}I_{ph}/\mathrm{d}t)]^{-1}. \tag{9}$$

From the slopes of I_{ph} versus time curves (in the decay region) (figures 8 and 9) and using equation (9), we have calculated the values of differential lifetime τ_d at various illumination times ($t = 30, 60, 90$ and 120 s). The results are plotted in figure 10. It is clear from the figure that τ_d increases with increase in exposure time. This confirms the non-exponential decay [33] in the present case; as for exponential decay, τ_d should be constant with time. The slow decay and long time constant can be explained in terms of trapping of charge carriers in the levels whose energetic depth from the conduction or valence band is large. So, recombination can be considered to take place through the valence or conduction band. The long time constant and slow decay can also be explained on the basis of band-to-band recombination via capture of an electron by the lattice defect [35]. The energy of a defect level depends on the relative position of the defect atom with respect to its surrounding lattice atoms. After the capture, the defect level moves up and down in the band gap about its equilibrium position, indicating very large relaxation. Therefore, in the decay process the differential lifetime becomes large. It has also been observed (figure 8) that, at $x = 5\%$, the photocurrent (in the decay region) decreases with increasing illumination time; this may be due to the defect states present in two different levels creating holes in the recombination process [36]. The photosensitivity σ_{ph}/σ_d is also calculated (table 1) at a particular intensity (108 lux) and at room temperature (287 K). The photosensitivity is very low for all the samples. The photosensitivity decreases with increasing Te concentration. The maximum photosensitivity is observed in binary $Se_{80}Ga_{20}$ only. The low photosensitivity reveals that thermally generated charge carriers recombine with majority charge carriers at a distance near the bottom of conduction band [37] in the $Se_{80-x}Te_xGa_{20}$ system. Here, it is interesting to explain this slow decay and low photosensitivity in terms of the density of the defect states. Hjartarson and Kao [38] made photoresponse measurements in the Se–Te system and concluded that the density of defect states increases by incorporation of Te. In the present system of a-$Se_{80-x}Te_xGa_{20}$, the density of defect states increases (table 3) and this increase in the density of defect states will consequently decrease the trap level, resulting in a low photosensitivity.

4. Conclusion

From the above results and discussion, one may conclude that hopping conduction is taking place in a-$Se_{80-x}Te_xGa_{20}$ (where $0 \leqslant x \leqslant 20$) over the entire temperature range of investigation. In the higher-temperature region (287–318 K), conduction takes place by

hopping of charge carriers in the tail states while, in the lower-temperature region (148–287 K), the conduction is due to variable-range hopping with a kink at a temperature of about 278 K, which is in fair agreement with the Mott condition of variable-range hopping conduction. Gallium gives a more pronounced effect on electrical conductivity as the Se–Te polymeric chain and Se–Te rings increase. The results of the transient photoconductivity observations show non-exponential decay. The recombination process in these glasses is taking place through the valence and conduction bands.

Acknowledgment

We are grateful to Professor Z H Zaidi for his valuable suggestions. Thanks are also due to UGC for financial assistance.

References

[1] Cheung L, Foley G M T and Springett B E 1982 *Photogr. Sci. Eng.* **26** 245
[2] Schottmiller J, Tabak M, Lucovsky G and Ward A 1970 *J. Non-Cryst. Solids.* 4 80
[3] Agarwal P, Rai J S P and Kumar A 1990 *Phys. Chem. Glasses* **31** 227
[4] Kolomiets B T and Goryunova N A 1955 *Zh. Tekh. Fiz.* **25** 984
[5] Goryunova N A and Kolomiets B T 1956 *Izv. Akad. Nauk SSSR, Ser. Fiz.* **20** 1496
[6] Danilov A V and Muller R L 1962 *Zh Prikl. Khim.* **35** 2012
[7] Kolomiets B T, Lebedev E A and Rogachev N A 1974 *Fiz. Tekh. Poluprov.* **8** 545
[8] Flasck R, Izu M, Sapru K, Anderson T, Ovshinsky S R and Fritzsche H 1977 *Proc. 7th Int. Conf. on Amorphous and Liquid Semiconductors* (Edinburgh: Centre of Industrial Consultancy and Liaison) p 624
[9] Okano S, Suzuki M, Imura K, Fukada N and Hiraki A 1983 *J. Non.-Cryst. Solids* **59–60** 969
[10] Manzar Malik M, Nigam A N and Husain M 1992 *X-ray Spectrom.* **21** 193–5
[11] Manzar Malik M, Zulfequar M, Kumar A and Husain M 1992 *J. Phys.: Condens. Matter* 4 8331–8
[12] Abkowitz M 1984 *Polym. Eng. Sci.* **24** 1149
[13] Mott N F 1970 *Phil. Mag.* **22** 7
[14] Mott N F and Davis E A 1970 *Phil. Mag.* **22** 903
[15] Mott N F and Davis E A 1970 *Electronic Processes in Non-Crystalline Materials* (Oxford: Clarendon) ch 9
[16] Twaddell V A, Lacourse W C and Mackenzie J D 1972 *J. Non-Cryst. Solids* **8–10** 831
[17] Mott N F 1975 *Phil. Mag.* **32** 961
[18] Mott N F 1969 *Phil. Mag.* **19** 835
[19] Lemoine D and Mendolia J 1981 *Phys. Lett.* **22A** 418
[20] Mishra R, Geol S, Tripathi S K, Agnihotri A K and Kumar A 1990 *Physica* B **167** 195–9
[21] Ray A K, Swan R and Hogarth C A 1994 *J. Non-Cryst. Solids* **168** 150–6
[22] Brodsky M H and Gambino R J 1972 *J. Non-Cryst. Solids* **8–10** 739
[23] Fritzsche H 1974 *Amorphous and Liquid Semiconductors* ed J Tauc (New York: Plenum) p 254
[24] Kumar S, Arora R and Kumar A 1992 *Solid State Commun.* **82** 725
[25] Onozuka A, Oda O and Tsuboya I 1987 *Thin Solid Films* **149** 9
[26] Knotek M L, Pollak M, Donovan T M and Kutzman H 1973 *Phys. Rev. Lett.* **30** 853
[27] Brodsky M H and Gambino R F 1972 *J. Non-Cryst. Solids* **8–10** 321
[28] Hauser J J 1972 *Phys. Rev. Lett.* **29** 476
[29] Mehra R M, Agarwal S C, Rani S, Shyam R, Agarwal S K and Mathur P C 1980 *Thin Solid Films* **71** 71
[30] Phahle A M 1977 *Thin Solid Films* **41** 35
[31] Mehra R M, Kumar H, Koul S and Kumar P 1984 *Mater. Chem. Phys.* **11** 481–94
[32] Igalson M 1982 *Solid State Commun.* **44** 247
[33] Fuch W and Mayer D 1974 *Phys. Status Solidi* a **24** 276
[34] Mathur R and Kumar A 1986 *Solid State Commun.* **59** 163
[35] Henry C H and Lang D V 1977 *Phys. Rev.* B **15** 989
[36] Stockmann F 1955 *Z. Phys.* **143** 348
[37] Rose A 1963 *Concepts in Photoconductivity* (New York: Interscience)
[38] Hjartarson G A and Kao K C 1984 *J. Mater. Sci. Lett.* **3** 253